ARKIV FÖR FYSIK Band 16 nr 5

Communicated 11 March 1959 by Erik Hulthén and Kai Siegbahn

Precision measurement of $K\alpha$ X-ray lines from rare earth elements

By Pär Bergvall

With 6 figures in the text

1. Introduction

Exact knowledge of the atomic level energies has become important not only in atomic and solid state physics, but also in nuclear spectroscopy. As it has been demonstrated in a previous report (1), the K-level energy of a heavier element is most accurately established by addition of the L_{III} (or L_{II}) level energy to the energy of the $K\alpha_1$ (or α_2) emission line. The latter figure is 5–8 times larger than the former, and the demands on the relative accuracy of the emission line determination are accordlingly much higher. With use of the precision, curved crystal spectrometer constructed at this institute, (2), it has been possible to obtain an absolute accuracy in the K emission line energies, comparable to the accuracy of the best L-level measurements available.

A systematic study of the K spectra of elements with atomic numbers higher than 50 was made in 1936 by Ingelstam (10). His error limits are only about twice the limits claimed for measurements with the present spectrometer, and his wavelength values have shown good agreement with recent determinations (2), (13). The rare earth elements, however, constitute a gap in Ingelstam's work, only the first four were measured by him. Other investigators had previously measured the K spectra of rare earth elements: Leide (11) in 1925 and Cork and Stephensson (8) in 1926. These measurements are, however, of much lower accuracy than those of Ingelstam's. In addition, Leide's measurements are nowadays believed to contain systematic errors. Cork and Stephensson's measurements are based on a value for the atomic spacing constant of calcite, different from the accepted value (14) and should be recalculated in order to be comparable with other determinations. Quite recently, in 1958, Chupp *et al.* (6) has investigated the K spectra of rare earths. This was done in connection with measurements of low energy nuclear transitions following Coulomb excitation in heavier elements. The spectrometer was of the curved crystal type in the Cauchois mounting with photographic registration. As reference lines the set of $K\alpha$ X-ray lines of the elements under investigation was used, employing wavelength values according to among others Ingelstam, Cork and Stephensson and the DuMond group. A gamma line in Ta^{182}, as measured by DuMond, was also used as reference. The calibration of the spectrometer was achieved by a least squares fit of all the reference lines to the experimental data. Wavelength values of all the measured lines (including the reference lines) were then obtained in terms of this calibration.

The details of the analysis are found in the reports (5) (6). Among the results are found wavelength values for the $K\alpha_1$ and α_2 lines of the last eight rare earth elements. The assigned error limits are, however, almost 10 times the limits given for measurements with the present spectrometer.

It is clear from the above that the precision measurements of $K\alpha$ lines of rare earth metals, reported below, fill a gap in the experimental data of X-ray spectroscopy. The K emission lines arising from transitions from the M and N levels have not been measured, however, as information of these level energies is preferably found in L and M emission spectra.

2. Experimental procedure

The X-ray source and the curved crystal spectrometer have been described in a previous report (2). The target plates, 20 mm in diameter, are screwed on to the water cooled, positive electrode of the X-ray tube. They were of the following description:

Mo. Solid metal plate, 2 mm thick.

La, Ce, Pr, Nd. The metals were rolled to a thickness of 0.2 mm and clamped on to copper target plates. These elements showed surface oxidation in air, and the surface was scraped clean before the insertion in the X-ray tube.

Sm, Gd, Tb, Dy, Ho, Er, Tm, Yb, Lu. The metals were evaporated to approximately $5\,\mu$ thick layers on to copper plates. These targets were prepared for us through Dr. Edward Chupp, University of California Radiation Laboratory, Livermore. All the deposits were black, evidently the metal oxides, and did not change during the experiments.

Eu. The oxide (Eu_2O_3) was evaporated on to a copper plate. The white oxide gave a black deposit. This was believed to be an oxide of lower valency.

The exact chemical nature of the thin targets was not established, as chemical effects on the $K\alpha$ emission lines can be considered negligible for these elements (13).

The X-ray tube was operated at 560 kV and 40 μA supplied by a van de Graaff generator. This gave sufficient counting rate even for the thin targets.

Before the measurements, a control of the spectrometer adjustments was undertaken. For the subsequent calibration the Mo $K\alpha_1$ line was used. One reason for the choice of this line is the fact that the large Bragg angle makes it possible to do the calibration with a high relative accuracy. A second reason is the suggestion by DuMond (12) to use this line for a new definition of the X unit. It was controlled after the completion of the measurements that the calibration had not changed.

A wavelength measurement with the spectrometer was carried out according to the following. The source slit was placed in the appropriate position to coincide with the Rowland circle for the actual wavelength region. The spectrometer was then set approximately on the peak of the spectral line, and a pulse height spectrum was recorded for the detector, a scintillation counter combined with a differential discriminator. Such a "monochromatic pulse spectrum" for La $K\alpha_1$ is shown in Fig. 1. The resolution is 53 %, but this figure decreases to 32 % for Lu $K\alpha_1$. With the detector channel set on the peak of the pulse spectrum, four independent line measurements, each consisting of delineations in the two positions of the spectrometer, were performed. The temperature was kept within 0.4° during a line measurement. Three typical spectrometer recordings are shown in Figs 2, 3, and 4. Fig. 2 is the Mo $K\alpha_1$

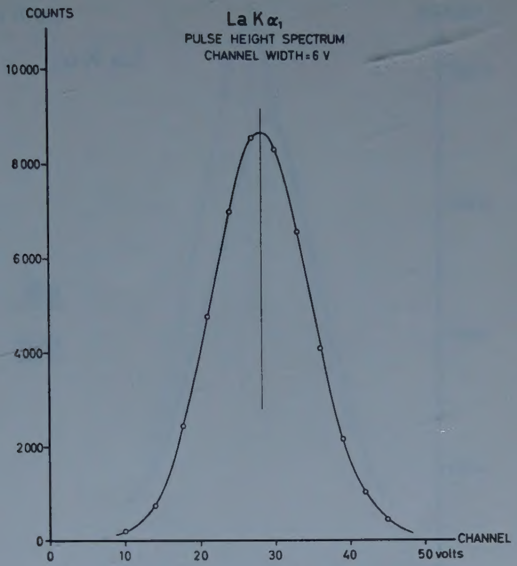

Fig. 1. Typical "monochromatic pulse spectrum" of the detector for low energy radiation, here 33.4 keV.

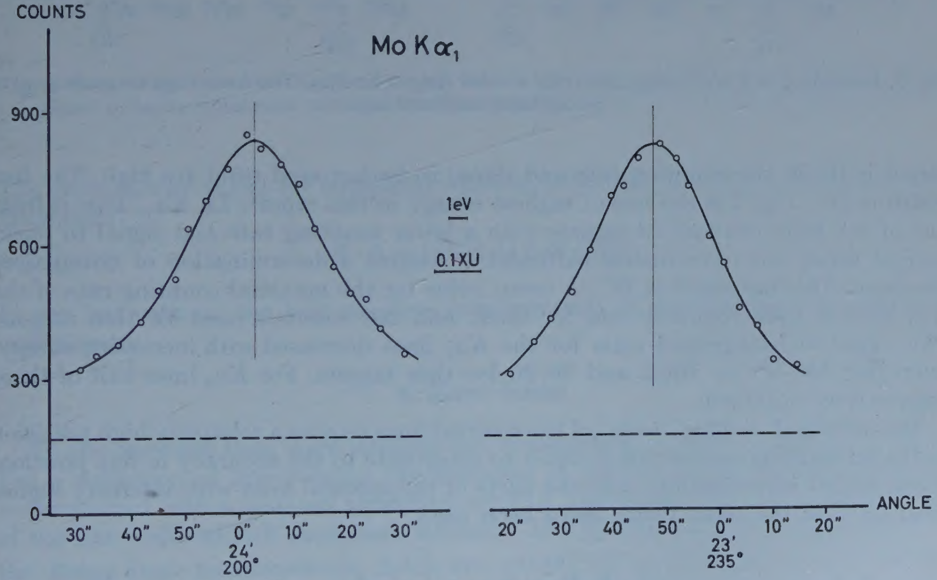

Fig. 2. The calibration line, Mo $K\alpha_1$, as recorded in the two spectrometer positions. The background is indicated by a dashed line.

line used for the calibration. Because of absorption, mainly in the quartz crystal, the counting rate and signal to background ratio are very low. This line is in fact the softest line we have been able to record with the instrument. The line width at half maximum is about 33″. Fig. 3 shows the first of the lanthanide lines, La $K\alpha_2$. The

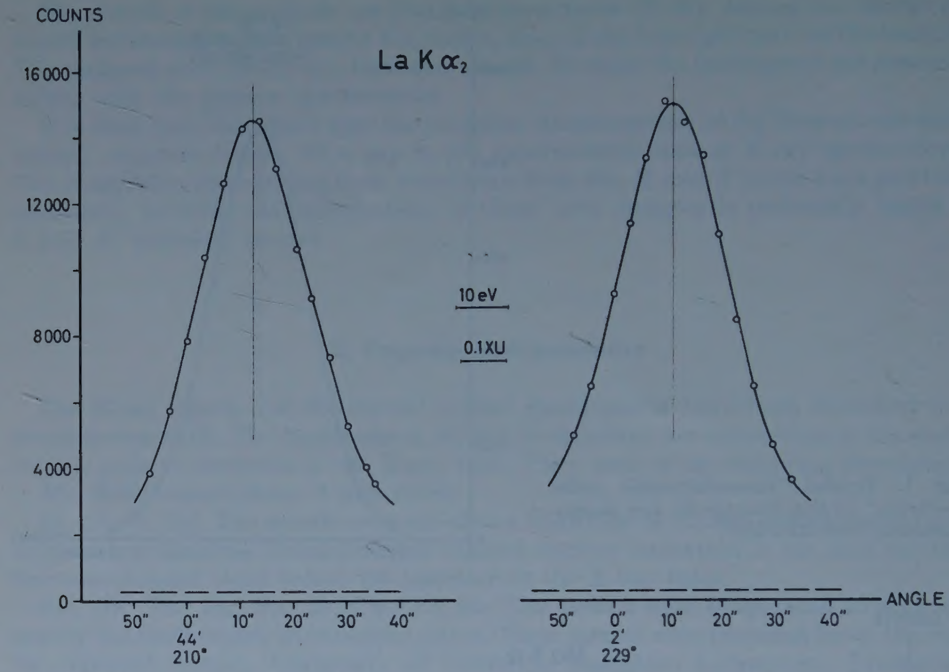

Fig. 3. Recording of a low energy line from a thick target, La $K\alpha_2$. The counting rate and signal to background ratio are high.

target is thick, the counting rate and signal to background ratio are high. The line width is 27″. Fig. 4 is the line of highest energy in this report, Lu $K\alpha_1$. This is from one of the thin, evaporated targets with a lower counting rate and signal to background ratio, but nevertheless sufficient to enable a determination of unimpaired precision. The line width is 25″. A mean value for the maximal counting rate of the $K\alpha_1$ lines is 1000 counts/second for thick, and 200 counts/second for thin targets. The signal to background ratio for the $K\alpha_1$ lines decreased with increasing energy, averaging 100–80 for thick and 30–20 for thin targets. For Ka_2 lines half of these figures were obtained.

The extended, sloping "tails" of the spectral lines require a relatively high precision in the intensity measurement in order to contribute to the accuracy in line position. Thus, in this investigation, only the parts of the spectral lines with intensity higher than 25 % of the peak value, have been used.

3. Experimental results

The results of the measurements are given in table 1. Bragg angles, given in the second column, have been reduced to 18°C (2). The mean Bragg angle, wavelength and energy, are given in the fourth column. Wavelength values, in X units, are calculated from the following wavelength value (13) of the calibration line:

Mo $K\alpha_1$: 707.831 XU.

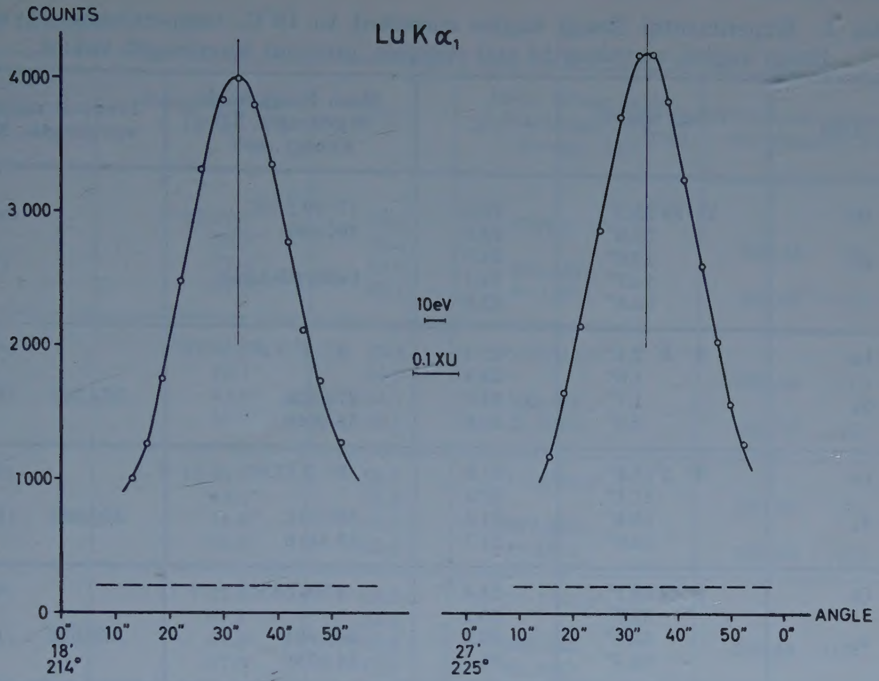

Fig. 4. Recording of the line of highest energy from a thin target, Lu $K\alpha_1$. The counting rate and signal to background ratio are considerably lower than in fig. 3, but still sufficiently high.

The given energy values are computed with use of the conversion factor of Cohen and DuMond (7):

$$E \cdot \lambda_s = 12372.44 \text{ keV} \cdot \text{XU}.$$

In the last column, the best previous measurements of wavelength are given for a comparison.

4. Error limits

All the recorded lines were straight and symmetrical within experimental errors. For a definition of line position the diameter of horizontal chords was used. This is determined with a *maximal* accidental error, Δ, estimated as $\pm 1/40$, for Mo $\pm 1/30$ of the line width at half maximum intensity. The corresponding statistical errors in the Bragg angle measurements, $\Delta/\sqrt{2}$, are $\pm 0.45''$ for La to Lu and $\pm 0.8''$ for Mo, in agreement with the maximal deviations from mean Bragg angles observed. As n independent measurements are made, ($n=4$ except for Mo), the accuracy of the mean is given by the expression:

$$\Delta/\sqrt{2n}.$$

This makes $\pm 0.23''$ for La to Lu and $\pm 0.36''$ for Mo.

Table 1. Experimental Bragg angles corrected to 18°C, temperatures (t), mean Bragg angles, wavelengths and energies, previous wavelength values.

Line	Bragg angles 18°C	t°C	Mean Bragg angle Wavelength, XU Energy, keV	Previous values, wavelength, XU
Mo α_1	17°29′25.5″ 26.3″ 25.6″ 24.7″ 25.5″	22.2 23.0 22.6 23.1 22.3	17°29′25.5″ **707.831** **Calibration line**	
La α_2	9° 9′ 2.4″ 1.6″ 1.7″ 2.0″	22.4 23.3 23.5 20.8	9° 9′ 1.9″ **374.536** 33.0340	374.522 (I)
La α_1	9° 2′17.4″ 17.1″ 16.8″ 16.6″	21.9 22.4 21.4 21.7	9° 2′17.0″ **369.971** 33.4416	369.962 (I)
Ce α_2	8°48′56.1″ 55.9″ 55.8″ 55.5″	24.4 25.1 23.0 23.7	8°48′55.8″ **360.934** 34.2789	360.936 (I)
Ce α_1	8°42′10.1″ 9.2″ 9.5″ 9.6″	24.4 22.3 25.1 23.9	8°42′ 9.6″ **356.350** 34.7199	356.355 (I)
Pr α_2	8°29′52.2″ 52.2″ 53.0″ 52.6″	23.3 23.8 21.9 22.5	8°29′52.5″ **348.028** 35.5501	348.025 (I)
Pr α_1	8°23′ 5.2″ 4.7″ 4.9″ 5.1″	22.5 22.0 22.7 23.4	8°23′ 5.0″ **343.426** 36.0265	343.428 (I)
Nd α_2	8°11′47.6″ 48.3″ 48.0″ 48.2″	22.6 23.0 23.5 23.8	8°11′48.0″ **335.777** 36.8472	335.768 (I)
Nd α_1	8° 4′59.3″ 59.7″ 59.5″ 59.5″	24.7 24.2 22.8 23.4	8° 4′59.5″ **331.159** 37.3610	331.153 (I)
Sm α_2	7°38′18.5″ 18.4″ 18.0″ 17.9″	23.2 23.2 23.2 23.5	7°38′18.2″ **313.048** 39.5226	313.02 (L) 313.24 (C)

Table 1 (cont.).

Line	Bragg angles 18°C	t°C	Mean Bragg angle **Wavelength, XU** Energy, keV	Previous values, wavelength, XU
Sm	7°31′27.7″	23.0	7°31′27.6″	
	27.3″	23.3		308.33 (L)
α_1	27.4″	22.8	**308.400**	
	27.9″	23.1	40.1181	308.58 (C)
Eu	7°22′45.5″	23.6	7°22′45.7″	
	46.1″	24.0		302.65 (L)
α_2	45.5″	24.1	**302.491**	
	45.6″	23.5	40.9018	302.73 (C)
Eu	7°15′53.9″	23.7	7°15′54.0″	
	54.2″	23.6		297.90 (L)
α_1	54.0″	23.2	**297.829**	
	53.8″	23.3	41.5421	298.03 (C)
Gd	7° 7′57.5″	23.5	7° 7′57.5″	
	57.1″	23.4		
α_2	57.5″	23.6	**292.431**	292.44 (Ch)
	57.8″	22.9	42.3089	
Gd	7° 1′ 4.8″	23.4	7° 1′ 4.9″	
	5.2″	24.0		
α_1	4.7″	24.1	**287.756**	
	4.9″	23.4	42.9963	287.75 (Ch)
Tb	6°53′51.2″	23.1	6°53′50.8″	
	50.6″	23.0		
α_2	50.7″	23.2	**282.836**	282.84 (Ch)
	50.8″	23.4	43.7443	
Tb	6°46′57.1″	24.1	6°46′57.2″	
	57.5″	23.7		
α_1	57.3″	23.8	**278.147**	
	56.9″	23.9	44.4817	278.14 (Ch)
Dy	6°40′23.1″	23.7	6°40′23.2″	
	23.0″	23.9		
α_2	23.6″	23.3	**273.679**	
	23.1″	23.3	45.2078	273.67 (Ch)
Dy	6°33′28.4″	23.1	6°33′28.4″	
	28.5″	23.8		
α_1	28.2″	23.8	**268.975**	
	28.5″	23.8	45.9985	268.96 (Ch)
Ho	6°27′32.2″	23.4	6°27′32.3″	
	32.5″	23.1		
α_2	32.5″	23.0	**264.936**	
	32.1″	23.7	46.6997	264.91 (Ch)

Table 1 (cont.).

Line	Bragg angles 18°C	t°C	Mean Bragg angle **Wavelength, XU** Energy, keV	Previous values, wavelength, XU
Ho	6°20′36.6″	22.9	6°20′36.4″	
	36.1″	23.1		
α_1	36.4″	23.2	**260.216**	
	36.5″	23.2	47.5469	260.19 (Ch)
Er	6°15′15.9″	20.9	6°15′15.8″	
	15.6″	20.9		
α_2	16.0″	21.0	**256.577**	
	15.7″	21.0	48.2212	256.55 (Ch)
Er	6° 8′18.5″	22.5	6° 8′18.7″	
	18.7″	20.7		
α_1	18.8″	18.0	**251.842**	
	18.7″	18.8	49.1278	251.82 (Ch)
Tm	6° 3′31.2″	21.9	6° 3′31.3″	
	31.3″	22.3		
α_2	31.4″	22.1	**248.579**	
	31.3″	23.2	49.7726	248.59 (Ch)
Tm	5°56′32.8″	22.8	5°56′33.2″	
	33.1″	22.7		
α_1	33.6″	22.8	**243.832**	
	33.4″	22.9	50.7417	243.79 (Ch)
Yb	5°52′16.9″	23.2	5°52′17.2″	
	17.3″	22.9		
α_2	17.3″	22.8	**240.924**	
	17.2″	22.8	51.3541	240.94 (Ch)
Yb	5°45′18.4″	22.0	5°45′18.2″	
	18.2″	22.1		
α_1	18.3″	22.8	**236.165**	
	18.0″	22.4	52.3891	236.16 (Ch)
Lu	5°41′31.8″	23.1	5°41′32.1″	
	32.2″	23.5		
α_2	32.3″	23.4	**233.596**	
	32.2″	23.7	52.9651	233.59 (Ch)
Lu	5°34′32.2″	22.4	5°34′32.1″	
	31.8″	22.8		
α_1	32.0″	21.5	**228.823**	
	32.3″	21.8	54.0698	228.81 (Ch)

C = Cork and Stephensson (8).
Ch = Chupp, DuMond, Gordon, Jopson, and Mark (6).
I = Ingelstam (10).
L = Leide (11).

Table 2. Assigned error limits. The errors are „±" values, and apply to both of the $K\alpha$ lines.

Element	XU	eV	Element	XU	eV	Element	XU	eV
La	0.004	0.4	Eu	0.004	0.5	Er	0.004	0.7
Ce	0.004	0.4	Gd	0.004	0.6	Tm	0.004	0.8
Pr	0.004	0.4	Tb	0.004	0.6	Yb	0.004	0.8
Nd	0.004	0.4	Dy	0.004	0.6	Lu	0.004	0.9
Sm	0.004	0.5	Ho	0.004	0.7			

To this is added (quadratically), 0.15″, estimated to account for none-linear systematic errors. In spite of the statistical nature of the above error, it should be kept in mind that Δ is a maximal error. It can be mentioned as a comparison that the root mean square deviation for the Bragg angle measurements in table 1 is ±0.2″. The standard deviation of 4 independent measurements is ±0.1″.

The error in mean Bragg angle according to the above is ±0.3″ for all the measurements except for Mo, where the error is ±0.4″. The latter gives rise to a calibration error of 6 ppm, which is included in the wavelength and energy error limits assigned. These are given in Table 2.

5. Discussion of results

It is difficult to find a systematic representation of the above results as a function of atomic number, doing full justice to all of the significant digits in the wavelength values. In the modified Moseley diagram, attributed to Idei (9), the square root of ν/R values is subtracted by a linear polynomial in Z, adjusted to give a minimum difference. For L levels and for K levels of lighter elements, one obtains in this way series of straight lines, showing discontinuities where new electron shells start to build up. For transitions between the levels, viz. X-ray emission lines, one obtains curves with no apparent discontinuities. The curvature increases for heavier elements. As a consequence, sufficient sharpness cannot be obtained by a linear "modification". Ingelstam (10), who first encountered this difficulty, used a polynomial of the third degree in Z which he subtracted from the $\sqrt{\nu/R}$ values. This method involves the disadvantage that the modified, difference curve aquires a complex form with maxima and minima of no physical significance. In the present work, a representation, similar to one used by Bäckström *et al.* (4), is chosen. Energies in keV are used instead of ν/R values, and the following expressions are calculated:

$$\begin{aligned} M(\alpha_1) &= \frac{\sqrt{E}}{Z} - (Z-57)\,0.001509 - 1.013940 \\ M(\alpha_2) &= \frac{\sqrt{E}}{Z} - (Z-57)\,0.001192 - 1.007700 \end{aligned} \qquad (1)$$

The result is shown in fig. 5. Error limits are indicated for a few points. Within these limits all the values fall on smooth curves. If one excepts systematic errors, such as a calibration error, this can be taken as a criterion on the accuracy of the measurements.

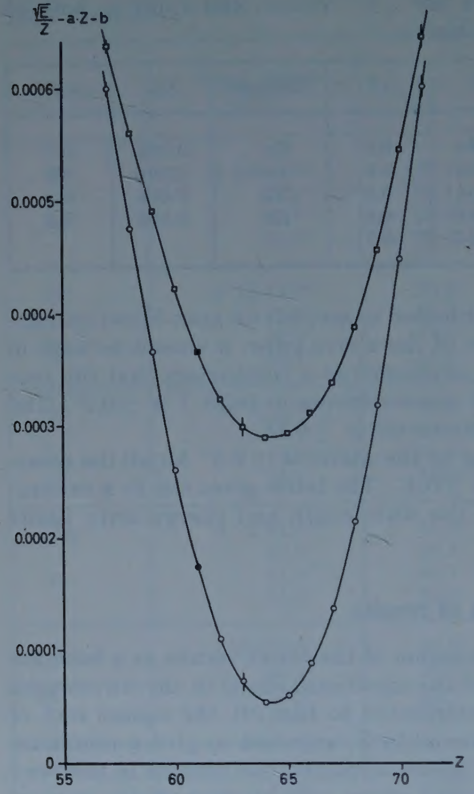

Fig. 5. Diagram showing the regularity in the variation of the $K\alpha$ line energies with atomic number. Upper curve: M (α_2) (□), lower curve: M (α_1) (O) according to eq. (1). The points for $Z = 61$ represent an interpolation.

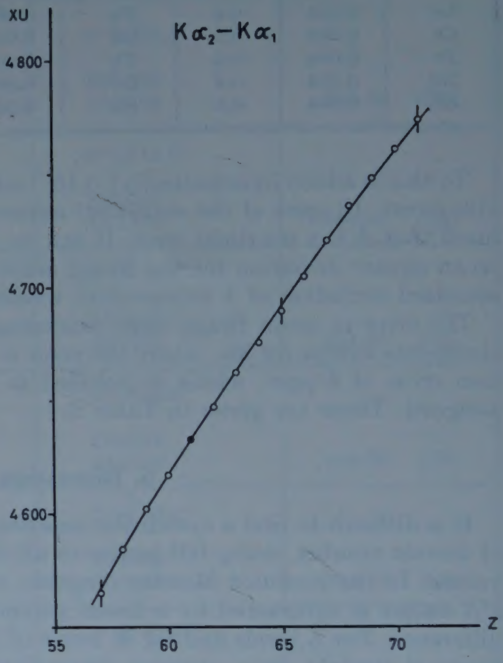

Fig. 6. The wavelength difference ($K\alpha_2 - K\alpha_1$) as a function of atomic number. The points follow a smooth curve well within experimental errors. The point for $Z = 61$ represents an interpolation.

The wavelength difference between the $K\alpha_2$ and the $K\alpha_1$ lines varies slowly and regularly with atomic number, and is well suited for a graphical representation. This is given in fig. 6. The wavelength difference is better determined than the absolute line wavelengths, as the close doublet lines are usually referred to almost the same set of five divisions on the circular scale. It is apparent, however, that the accidental errors in the line measurements are well within the estimated error limits. As expected, no apparent discontinuity is caused in either of the above diagrams by the fact that the first four elements were in metallic form, whereas the rest were oxides.

The energy difference in electron volts, viz. the energy difference between the L_{II} and L_{III} levels, is not suited for a diagram of the above kind. It is of interest, however, to compare the present results with previous data on this difference, obtained from L emission spectra. Such a comparison is seen in table 3, where data according to Sandström (13) are given, calculated from ν/R values with use of the

Table 3. L_{II}–L_{III} energy difference, in eV.

Element	Present	Reference (13)
La	407.6	407.6
Ce	441.0	441.0
Pr	476.4	475.9
Nd	513.8	513.2
Sm	595.6	605.5
Eu	640.3	639.2
Gd	687.4	687.3
Tb	737.4	737.1
Dy	790.7	791.8
Ho	847.1	844.6
Er	906.6	906.5
Tm	969.1	967.2
Yb	1035.0	1035.5
Lu	1104.7	1104.2

conversion factors according to Cohen and DuMond (7), used in the present work. The agreement is in most cases very good, and the larger deviations which occur are probably due to errors in the previous measurements.

Promethium

Element number 61, having no stable isotope, is not included in the experimental part of this work for obvious reasons. Its K spectrum has been measured by Buckhart, Peed and Spitzer (3). The wavelength values given for the $K\alpha$ lines are apparently greatly in error, and it seems appropriate to make use of the present data for an interpolation. This was done by taking first and second differences of the $\sqrt{E}$ values. This gave good agreement with graphical interpolation in the diagram of figure 5. The energy difference of the α_1 and α_2 values obtained fits very nicely into the diagram of figure 6. It does not appear too improper to assign the same error limits as to the nearby measurements.

Table 4. Promethium, interpolated values.

Line	Wavelength, XU	Energy, keV	Buckhart *et al.*, XU
$K\alpha_2$	324.130	38.1713	323.73
$K\alpha_1$	319.497	38.7247	319.06

Errors: ±0.004 XU, ±0.5 eV.

SUMMARY

Precision measurements of the $K\alpha_1$ and α_2 X-ray lines of rare earth elements are reported. The accuracy in the wavelength determination is given as 0.004 XU. Good agreement is obtained with L_{II}–L_{III} level differences obtained from L spectra. An interpolation of element 61 is given, making the list of elements 57–71 complete.

ACKNOWLEDGEMENTS

I am much indebted to Dr. Olof Beckman for his constant support and valuable advice. I am also deeply grateful to Dr. Edward L. Chupp and co-workers, University of California Radiation Laboratory, for the generous gift of ten rare earth targets, specially prepared for this investigation. Sincere thanks are due Fil. mag. Nisse Gidlöf for skilful operation of the van de Graaff generator and Mr. William Parker for preparation of some of the targets.

Institute of Physics, Uppsala, Sweden.

REFERENCES

1. Beckman, O., Axelsson, B., and Bergvall, P., Arkiv f. Fysik *15*, 567 (1959).
2. Beckman, O., Bergvall, P., and Axelsson, B., Arkiv f. Fysik *14*, 419 (1958).
3. Buckhart, L. E., Peed, W. F., Spitzer, E. J., Phys. Rev. *75*, 86 (1949). See also comment in ref. (13).
4. Bäckström, G., Bergman, O., and Burde, J., Nuclear Physics *7*, 263 (1958).
5. Chupp, E. L., DuMond, J. W. M., Gordon, F. J., Jopson, R. C., and Mark, H., Phys. Rev. *112*, 518 (1958).
6. Chupp, E. L., DuMond, J. W. M., Gordon, F. J., Jopson, R. C., and Mark, H., Phys. Rev. *112*, 1183 (1958).
7. Cohen, E. R., and DuMond, J. W. M., Handbuch der Physik, S. Flügge, Bd. XXXV (1957), or Cohen, E. R., DuMond, J. W. M., Layton, T. W., and Rollett, J. S., Rev. Mod. Phys. *27*, 363 (1955).
8. Cork, J. M., and Stephensson, B. R., Phys. Rev. *27*, 530 (1926).
9. Idei, S., Sci. Rep. Tôhoku Univ. ser. I *19*, 559 (1930).
10. Ingelstam, E., Nova Acta Reg. Soc. Sc. Ups. ser. IV, *10* (1936).
11. Leide, A., Diss. Lund 1925, or Comptes Rendus *180*, 1203 (1925).
12. Merrill, J. J., and DuMond, J. W. M., Phys. Rev. *110*, 79 (1958).
13. Sandström, A. E., Handbuch der Physik, S. Flügge, Bd XXX (1957).
14. Siegbahn, M., Spektroskopie der Röntgenstrahlen, 2 Aufl., Berlin 1931.

Tryckt den 26 juni 1959

Uppsala 1959. Almqvist & Wiksells Boktryckeri AB